Available online at www.sciencedirect.com
SCIENCE DIRECT®
Journal of the European Ceramic Society 25 (2005) 227–231
www.elsevier.com/locate/jeurceramsoc

Coarsening of nano-crystalline SiC in amorphous Si–B–C–N

H. Schmidt[a,*], W. Gruber[a], G. Borchardt[a], P. Gerstel[b], A. Müller[b], N. Bunjes[c]

[a] *TU Clausthal, FB Physik, Metallurgie und Werkstoffwissenschaften, AG Thermochemie und Mikrokinetik, Robert-Koch-Str. 42, D-38678 Clausthal-Zellerfeld, Germany*
[b] *Max-Planck-Institut für Metallforschung and Institut für Nichtmetallische Anorganische Materialien, Universität Stuttgart, Pulvermetallurgisches Laboratorium, Heisenbergstr. 3, D-70569 Stuttgart, Germany*
[c] *Max-Planck-Institut für Metallforschung, Abt. Mikrostruktur und Gefüge, Heisenbergstr. 3, D-70569 Stuttgart, Germany*

Available online 11 September 2004

Abstract

The formation of nano-crystalline SiC is studied in various amorphous precursor derived Si–B–C–N bulk ceramics at temperatures between 1600 and 1800 °C. The formation process of SiC can be described by a very rapid crystallization (<15 min) of nano-sized particles with diameters between 2 and 7 nm which are embedded in an amorphous Si–B–C–N matrix. During further annealing of the material up to 40 h, particle growth due to coarsening takes place, which leads to maximum crystallite diameters of 30 nm. The kinetics of coarsening can be described by the Lifshitz–Slyozov–Wagner model. The product of the rate constant of coarsening, k_c, and of the temperature, T, follows an Arrhenius behaviour with an activation enthalpy of about 8 eV (770 kJ/mol), which is approximately the activation enthalpy of self-diffusion in Si–B–C–N, indicating diffusion controlled crystallite growth. The kinetics of coarsening is fastest for the ceramics with a low concentration of Si and N in the amorphous matrix.

Keywords: Metastable material; Thermolysis; Ammonolysis

1. Introduction

Si–B–C–N ceramics derived from polymer precursors attract attention due to their outstanding high temperature stability up to 2000 °C[1–5] and their excellent mechanical properties.[6–8] Amorphous, thermodynamically metastable material can be prepared by solid state thermolysis at temperatures between 1000 and 1400 °C. Annealing at higher temperatures in an inert atmosphere leads to complete or partial crystallization of silicon carbide and silicon nitride, yielding different types of composites (e.g. nano-crystalline/amorphous). Thus, in order to obtain an optimized stability of the amorphous state for technological applications and to produce tailor-made microstructures, it is necessary to investigate and understand the formation of nano-sized crystallites during crystallization and their kinetics on the basis of the underlying atomic transport processes.

In the present study, we investigated the formation of nano-crystalline SiC in bulk ceramics with three different chemical compositions obtained from different processing routes as a function of annealing time and temperature. X-ray diffractometry (XRD) and transmission electron microscopy (TEM) were used to obtain information on the mechanisms and kinetics of particle growth.

2. Experimental procedure

Three types of ceramics were investigated, which will be referred to as materials T21, MW33, and AM26. The bulk samples under investigation were produced by uniaxial warm-pressing (300–400 °C, 40–50 MPa) and subsequent thermolysis (1000–1400 °C) of cross-linked preceramic polymers in an argon atmosphere. The Si–B–C–N ceramics T21 and MW33 were produced from different boron modified polysilazanes, on different reaction pathways. The T21 precursor[1] was obtained by hydroboration of dichloromethylvinylsilane and subsequent ammonolysis

* Corresponding author. Tel.: +49 53 2372 2094; fax: +49 53 2372 3184.
E-mail address: harald.schmidt@tu-clausthal.de (H. Schmidt).

0955-2219/$ – see front matter © 2004 Elsevier Ltd. All rights reserved.
doi:10.1016/j.jeurceramsoc.2004.08.004

Table 1
Chemical composition after thermolysis, calculated average composition of the amorphous matrix after crystallization, fraction of crystallized SiC phase *f*, and activation enthalpy of coarsening ΔH^c for various Si–B–C–N ceramics

Materials name	Chemical composition (at.%)	Calculated matrix composition (at.%)	*f* (%)	ΔH^c (kJ/mol)	ΔH^c (eV)
MW33	$Si_{25}B_9C_{39}N_{27}$	$Si_{19}B_{11}C_{36}N_{34}$	20	800 ± 100	8.3 ± 1
T21	$Si_{29}B_{10}C_{42}N_{19}$	$Si_{22}B_{13}C_{40}N_{25}$	25	820 ± 100	8.5 ± 1
AM26	$Si_{13}B_{13}C_{61}N_{13}$	$Si_4B_{16}C_{64}N_{16}$	20	700 ± 60	7.2 ± 0.6

(monomer route) while the MW33 polymer (*1P* in Weinmann et al., 2000)[9] was prepared via ammonolysis of dichlorovinylsilane followed by hydroboration (polymer route). The AM26 precursor was derived from bis(trivinylsilyl)carbodiimide by complete hydroboration of the vinyl groups (polymer 5 in Müller et al., 2002).[10] The approximate chemical composition after thermolysis is given in Table 1.

To observe the formation of SiC, the bulk ceramics were annealed in nitrogen (980 mbar) in the temperature range between 1600 and 1800 °C for times up to 50 h. Investigations with XRD were carried out with a SIEMENS D5000/Kristalloflex diffractometer in the θ–2θ modus using Co Kα radiation (40 kV, 40 nA) on bulk ceramics. An adjustable sample holder was used to position the sample surface reproducibly in the incidence plane of the X-rays. Coarse grained silicon carbide powder used as a reference material discarded any relevant influence of instrumental broadening on crystallite size analysis for the present measurements. Characterization with TEM was carried out with a Zeiss EM912 microscope equipped with an Omega energy-filter operating at 120 keV.

3. Results and discussion

Fig. 1(a) shows exemplarily the X-ray diffractograms of Si–B–C–N ceramics of type T21, MW33, and AM26 in the as-thermolysed state and after annealing for 2 h at 1800 °C. The as-thermolysed samples did not reveal any distinct X-ray reflections, confirming the amorphous nature of the material which was proven by TEM and selected area diffraction.[11] Annealing in the temperature range between 1600 and 1800 °C in nitrogen leads to the formation of broad reflections at Bragg angles of $2\theta = 41.7$, 71.2, and 86.0° which become more pronounced for higher annealing temperatures. This indicates the formation of nano-sized SiC crystallites within an amorphous Si–B–C–N matrix. The very broad maximum at around $2\theta = 29°$ is reminiscent of a graphite-like amorphous phase.[12] From the XRD patterns the approximate fraction of crystallized SiC phase is calculated to be about 25% (T21), 20% (MW33), and 20% (AM26), in acceptable accordance with thermodynamic calculations.[13,14] Annealing of the T21 and MW33 ceramics for prolonged times leads to the formation of β-Si_3N_4 in an additional crystallization step. In this study we focus on the crystallization and growth behaviour of SiC, whereby the formation of Si_3N_4 will be published elsewhere.[15] The maximum annealing times for which we detect only crystalline SiC and no significant fractions of crystalline Si_3N_4 are 40 h at 1600 °C, 15 h at 1700 °C, and 2 h at 1800 °C for both materials. For the AM26 material no additional formation of secondary crystalline phase is observed for the temperatures and times measured.

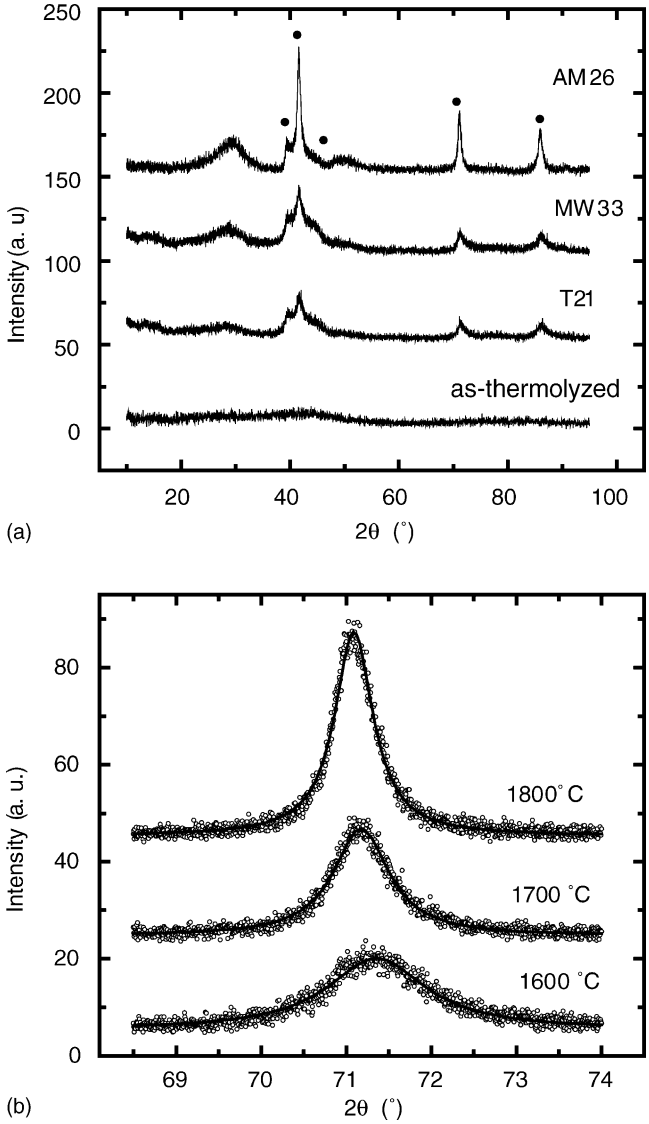

Fig. 1. (a) X-ray diffractograms of various Si–B–C–N ceramics in the as-thermolysed state and after annealing for 2 h at 1800 °C. The Bragg peaks corresponding to the SiC phase are indicated by a circle. (b) The SiC Bragg peak at an angle of 71.2° for the AM26 material after annealing for 2 h at temperatures between 1600 and 1800 °C. The solid line corresponds to a least-square fit of the data to a Lorentzian function, wherefrom the integrated peak area $I(t)$ and the full-width at half-maximum $\beta(2\theta)$ are determined.

For further analysis, all SiC peaks were numerically fitted with a Lorentzian function, from which the integrated peak area $I(t)$ and the full width at half maximum $\beta(2\theta)$ of the corresponding peak were determined (Fig. 1(b)). With XRD it is possible to determine the average volume-weighted diameter of crystals $\langle d \rangle$ (for definition, see, e.g. Natter et al., 1996)[18] from $\beta(2\theta)$ with the Scherrer formula:[16]

$$\langle d \rangle = \frac{0.9\lambda}{\beta(2\theta)\cos\theta}, \quad (1)$$

where $\lambda = 0.1789$ nm is the wave length of the Co tube radiation. Using the Bragg peak at $2\theta = 71.2^\circ$, which shows no overlap with neighbouring reflections, and Eq. (1) for analysis, crystallite diameters between 2 and 30 nm are determined, depending on the type of material, the temperature and the annealing time. An analysis of the XRD diffractograms with the Williamson–Hall method[17] at 1800 °C, where the single SiC peaks are relatively well separated, yielded no significant hint on a possible contribution of microscopic strain to profile broadening. As shown in Fig. 2(a) investigations with TEM on AM26 material revealed that the SiC precipitates are approximately nano-sized spheres embedded in an amorphous, turbostratic host matrix. From image analysis of the TEM micrograph in Fig. 2(a) the particle distribution of the SiC crystallites is obtained, as shown in Fig. 2(b). The particle distribution function can be fitted in good approximation by a log–normal function with a maximum value at a diameter of 12 nm. An average volume-weighted crystal diameter of 29 ± 3 nm is derived, which is in good accordance with the value of 25 ± 3 nm obtained from the present XRD measurements, justifying the application of X-ray diffractometry for the determination of crystallite diameters.

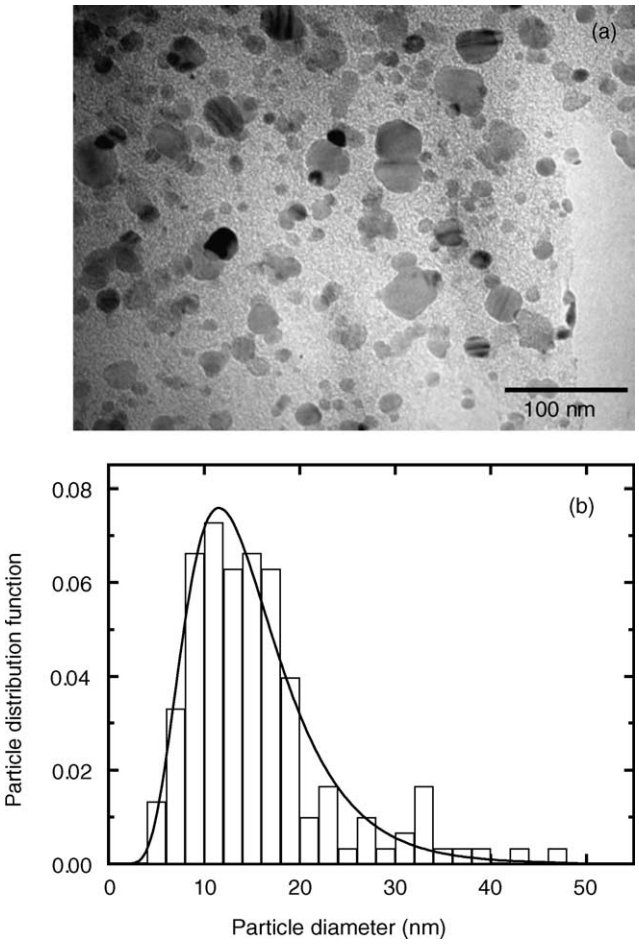

Fig. 2. (a) TEM micrograph taken from a AM26 sample after annealing for 5 h at 1800 °C. The dark spheres correspond to nano-crystalline SiC which is embedded in a turbostratic BNC_x matrix. (b) The particle distribution as determined from the TEM micrograph. The solid line is a least-square fit of a log–normal distribution function to the data.

To analyse the detailed kinetics of SiC formation the following procedure was applied: first, the amorphous ceramics were annealed at a distinct temperature in the range between 1600 and 1800 °C for a given time t_a. Then the films were characterized with XRD and afterwards annealed again. The annealing time dependence of the integrated peak area $I(t)$, which is proportional to the crystallized volume fraction $\chi(t)$ and the average crystallite diameter $\langle d \rangle$ are displayed in Fig. 3 for a T21 ceramic at 1700 °C as a typical example. It can be seen that with increasing annealing time $I(t)$ is nearly unchanged while $\beta(2\theta)$ is broadening continuously. This behaviour is observed at every annealing temperature for all Si–B–C–N samples investigated.

In general, the formation of a crystalline phase (SiC) out of a supersaturated amorphous matrix (Si–B–C–N) by de-mixing and crystallization occurs by the processes of nucleation, growth, and coarsening. The progress of this transformation can be tracked by monitoring the mean crystallite radius $\langle r \rangle(t)$ and the crystallized volume fraction $\chi(t)$. The classical nucleation and growth process is governed by an increase of the crystallized volume fraction and the average crystallite radius with time, while for coarsening only the average crystallite radius grows with time and the crystallized volume fraction remains constant. From this we conclude that the observed time dependent growth process of SiC is due to coarsening, where large crystallites grow slowly at the expense of small ones without a change in the overall volume fraction. As a consequence, the intrinsic nucleation and growth process taking place prior to coarsening has to be very fast. It happens within the first 15 min (shortest possible annealing time) of the annealing procedure at temperatures between 1600 and 1800 °C and can not be resolved with the present experimental equipment.

For spherically shaped crystallites, diffusion controlled coarsening can be described by a theory developed simultaneously by Lifshitz and Slyozov[19] and Wagner[20] (LSW theory). Here, the growth process is driven by a reduction of the overall interfacial energy between crystallite and amorphous matrix. The average crystallite radius at time t is given by:

$$\langle r \rangle^3(t) = r_0^3 + k_c t, \quad (2)$$

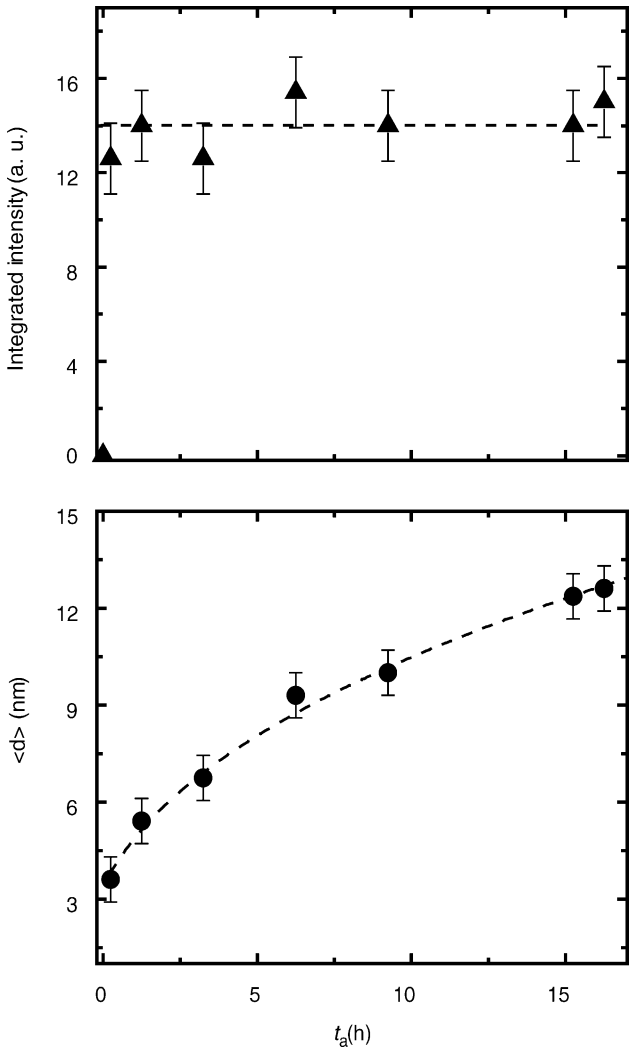

Fig. 3. The integrated peak intensity (which is proportional to the crystallized SiC fraction) and the average SiC crystallite diameter as obtained from the SiC Bragg peak at an angle of 71.2° as a function of annealing time at 1700 °C for the T21 material. The dotted lines are a guide to the eye.

where r_0 is the crystallite radius at the beginning of the coarsening process and k_c is the temperature dependent rate constant of coarsening. As an example, in Fig. 4 data of the AM26 material are plotted as $\langle r\rangle^3$ versus t for consistency with Eq. (2) at different temperatures. All type of Si–B–C–N ceramics investigated in this study show in good approximation a $\langle r\rangle^3$-behaviour, indicating the validity of the LSW theory. The rate constants were determined from the slope of the linear fits. According to the LSW theory the rate constant k_c can be described as:[21]

$$k_c = D\frac{8\gamma V_m c_m(1-c_m)}{9RT(c_c-c_m)^2} \tag{3}$$

for an ideal solid solution, where c_m is the solubility of Si in the amorphous matrix, c_c is the solubility in SiC, V_m is the molar volume of SiC, D is the diffusivity of the slowest component in the matrix, γ is the interfacial energy, and R is the gas constant. Under the assumption that the solubility in

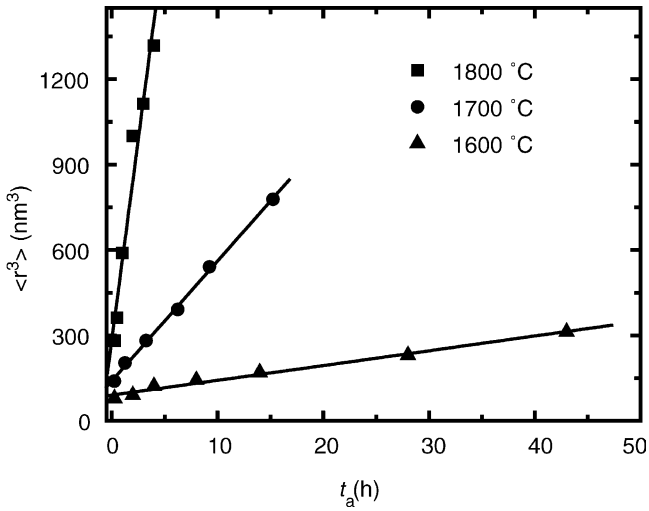

Fig. 4. Cube of the average grain radius $\langle r\rangle$ as a function of annealing time, t_a, at different temperatures for the AM26 material. The solid lines are least square fits according to Eq. (2).

the matrix, c_m, depends only weakly on temperature for $T \leq 1800\,^{\circ}\mathrm{C}$, the diffusivity,

$$D = D_0 \exp\left(-\frac{\Delta H^d}{k_B T}\right), \tag{4}$$

is the only significant temperature dependent quantity on the right side of Eq. (3). A plot of $\log(k_c T)$ versus $1/T$ (Fig. 5) should result in a straight line from which the activation enthalpy of coarsening ΔH^c can be determined and which should be identical to the activation enthalpy of diffusion ΔH^d. Indeed, straight lines are obtained for all three materials. The determined activation enthalpies of coarsening

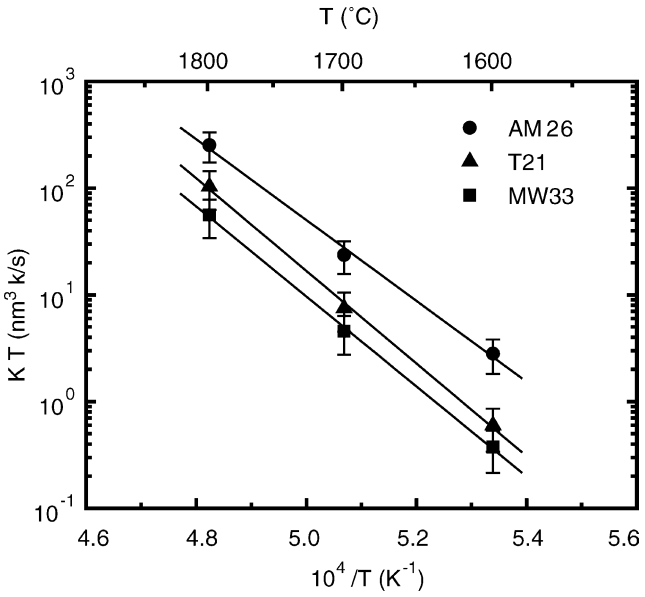

Fig. 5. Plots of $\log(k_c T)$ vs. $1/T$ describing the coarsening of SiC in Si–B–C–N.

are given in Table 1. Very high values in the order of 8 eV (770 kJ/mol) are obtained, showing not much variation for the three ceramics within error bars.

Experiments on self-diffusion of Si, C and N in amorphous Si–(B–)C–N ceramics of type T21 were carried out by our group with stable isotopes by means of secondary ion mass spectrometry.[22–24] The results exhibited a thermally activated behaviour in analogy to crystalline materials. Only small differences between the diffusivities of the three elements were measured (about one order of magnitude) indicating that the growth processes are influenced by all elements equally. Activation enthalpies in the order of ΔH^{d} = 6–7 eV (580–680 kJ/mol) are observed, which roughly coincide with the activation enthalpies of coarsening within error bars. From these data we conclude that the coarsening behaviour of SiC in Si–B–C–N is controlled by diffusion. The slightly lower value of ΔH^{d} (about 1 eV) compared to ΔH^{c} for the T21 and MW33 materials can be attributed to the fact that in our experiments tracer diffusivities are measured and not chemical diffusivities, which may differ. A non-negligible temperature dependence of the Si solubility in Si–B–C–N may also be responsible for the deviations.

As shown in Fig. 5, the rate constants of the MW33 material are lowest, while those for the T21 and AM26 material are larger by a factor of about 2 and 6, respectively. During crystallization of SiC the composition of the amorphous matrix is modified while an enrichment of nitrogen and boron and a depletion of silicon and carbon takes place. At the end of the crystallization process (and at the beginning of the coarsening process) we calculated a modified matrix composition using the fraction of crystallized phase and assuming conservation of atom numbers (Table 1). We see that the coarsening, and consequently the underlying self-diffusion processes in the matrix are fast for low silicon and nitrogen concentrations. As a result, we find from the present investigation that an increased fraction of Si and N in the amorphous matrix reduces the coarsening of SiC crystallites. The AM26 material, where nearly no additional Si_3N_4 crystallizes at long annealing times exhibits the largest rate constant.

4. Conclusion

In this study we presented an experimental investigation on the crystallization and coarsening of SiC in various amorphous Si–B–C–N ceramics derived from pre-ceramic polymers by thermolysis. Our main results are resumed as follows: (1) Isothermal heat treatment in the temperature range between 1600 and 1800 °C leads to a very rapid (<15 min) thermally activated crystallization process and to the formation of nano-crystalline SiC, embedded in an amorphous host matrix. (2) Further annealing leads to particle growth by coarsening according to the LSW theory, until additional silicon nitride is formed. (3) The product of the coarsening rate constant and the temperature follows a thermally activated behaviour with a large activation enthalpy of about 8 eV (770 kJ/mol). Comparison with self-diffusion data indicates a diffusion controlled coarsening process in Si–B–C–N. (4) The kinetics of coarsening is fastest for the ceramics with a low concentration of Si and N in the amorphous matrix.

Acknowledgements

The authors would like to thank M. Weinmann and J. Bill for supplying precursor ceramics, M. Rühle for access to the TEM facilities, and E. Ebeling for ceramographic preparation of the samples. This work has been funded by the Deutsche Forschungsgemeinschaft (DFG).

References

1. Riedel, R., Kienzle, A., Dressler, W., Ruwisch, L., Bill, J. and Aldinger, F., *Nature*, 1996, **382**, 796.
2. Aldinger, F., Weinmann, M. and Bill, J., *Pure Appl. Chem.*, 1998, **70**, 439.
3. Bill, J. and Aldinger, F., *Z. Metallkd.*, 1996, **87**, 827.
4. Müller, A., Gerstel, P., Weinmann, M., Bill, J. and Aldinger, F., *J. Eur. Ceram. Soc.*, 2001, **21**, 2171.
5. Jansen, M., *Solid State Ionics*, 1997, **101**, 1.
6. Zimmermann, A., Bauer, A., Christ, M., Cai, Y. and Aldinger, F., *Acta Mater.*, 2002, **50**, 1187.
7. Christ, M., Thurn, G., Weinmann, G., Bill, J. and Aldinger, F., *J. Am. Ceram. Soc.*, 2000, **83**, 3025.
8. Riedel, R., Ruwisch, L., An, L. and Raj, R., *J. Am. Ceram. Soc.*, 1998, **81**, 3341.
9. Weinmann, M., Schuhmacher, J., Kummer, H., Prinz, S., Peng, J., Seifert, H. J. *et al.*, *Chem. Mater.*, 2000, **12**, 623.
10. Müller, A., Gerstel, P., Weinmann, M., Bill, J. and Aldinger, F., *Chem. Mater.*, 2002, **14**, 3398.
11. Cai, Y., Zimmermann, A., Prinz, S., Zern, A., Phillipp, F. and Aldinger, F., *Scr. Mater.*, 2001, **45**, 1301.
12. Haug, J., Lamparter, P., Weinmann, M. and Aldinger, F., *Chem. Mater.*, 2004, **16**, 83.
13. Peng, J., Thermochemistry and constitution of precursor-derived SI–B–C–N ceramics. Ph.D. thesis, University of Stuttgart, Germany, 2002.
14. Müller, A., Peng, J., Seifert, H. J., Bill, J. and Aldinger, F., *Chem. Mater.*, 2002, **14**, 3406.
15. Schmidt, H., Gruber, W. and Borchardt, G., unpublished.
16. Scherrer, P., *Göttinger. Nachr. Math. Phys.*, 1918, **2**, 98.
17. Williamson, G. K. and Hall, W. H., *Acta Mater.*, 1953, **1**, 22.
18. Natter, H., Krajewski, T. and Hempelmann, R., *Ber. Bunsenges. Phys. Chem.*, 1996, **100**, 55.
19. Lifshitz, I. M. and Slyozov, V. V., *Phys. Chem. Solids*, 1961, **19**, 35.
20. Wagner, C., *Z. Elektrochem.*, 1961, **65**, 581.
21. Calderon, H. A., Voorhees, P. W., Murray, J. L. and Kostorz, G., *Acta Metall. Mater.*, 1994, **42**, 991.
22. Schmidt, H., Borchardt, G., Weber, S., Scherrer, S., Baumann, H., Müller, A. *et al.*, *J. Appl. Phys.*, 2000, **88**, 1827.
23. Schmidt, H., Borchardt, G., Weber, S., Scherrer, H., Baumann, H., Müller, A. *et al.*, *J. Non-Cryst. Solids*, 2002, **298**, 232.
24. Schmidt, H., Borchardt, G., Baumann, H., Weber, S., Scherrer, S., Müller, A. *et al.*, *Def. Diff. For.*, 2001, **194–199**, 941.